colloids and interfaces

MDPI

Article

Bio-Based Interpolyelectrolyte Complexes for the Stabilization of Pickering-like Emulsions

Francisco Joel Guerrero-Vasquez [1], Francisco Ortega [1,2], Ramón G. Rubio [1,2] and Eduardo Guzmán [1,2,*]

[1] Departamento de Química Física, Facultad de Ciencias Químicas, Universidad Complutense de Madrid, Ciudad Universitaria, Plaza de la Ciencias s/n, 28040 Madrid, Spain; frangu02@ucm.es (F.J.G.-V.); fortega@quim.ucm.es (F.O.); rgrubio@quim.ucm.es (R.G.R.)
[2] Instituto Pluridisciplinar, Universidad Complutense de Madrid, Paseo Juan XXIII 1, 28040 Madrid, Spain
* Correspondence: eduardogs@quim.ucm.es; Tel.: +34-91-394-4107

Abstract: This work studies the stabilization of Pickering-like emulsions using dispersions of interpolyelectrolyte complexes (IPECs) formed by chitosan (CS) and sodium alginate (ALG), two polymers from natural resources, as the aqueous phase and soybean oil as the oil phase. The ability of these bio-based IPECs to form stable emulsions was evaluated by varying the compositional ratio of CS to ALG (*Z*-ratio) and the oil volume fraction (ϕ_o). Turbidity, zeta potential, and dynamic light scattering measurements revealed the dependence of IPEC properties on the *Z*-ratio, with phase separation observed near stoichiometric ratios. Phase diagram analysis showed that stable oil-in-water (O/W) and water-in-oil (W/O) emulsions could be obtained under certain combinations of the *Z*-ratio and ϕ_o. Emulsion stability increased with higher *Z*-ratios due to increased interfacial activity of the complexes and reduced coalescence. Emulsions with high ϕ_o exhibited transitions from discrete droplets to bicontinuous interfacially jammed emulsion gels (bijels), suggesting tunable morphologies. These results highlight the potential of CHI-ALG IPECs as eco-friendly and efficient stabilizers of Pickering-like emulsions for applications in food, cosmetics and pharmaceuticals.

Keywords: chitosan; interpolyelectrolyte complexes; Pickering emulsions; sodium alginate; soybean oil

Academic Editor: Thodoris Karapantsios

Received: 19 December 2024
Revised: 17 January 2025
Accepted: 21 January 2025
Published: 22 January 2025

Citation: Guerrero-Vasquez, F.J.; Ortega, F.; Rubio, R.G.; Guzmán, E. Bio-Based Interpolyelectrolyte Complexes for the Stabilization of Pickering-like Emulsions. *Colloids Interfaces* **2025**, *9*, 9. https://doi.org/10.3390/colloids9010009

1. Introduction

Emulsions, mixtures of two immiscible liquids stabilized by emulsifiers, play an important role in many areas including food, pharmaceuticals, cosmetics and materials science. Conventional emulsions typically rely on the use of surfactants to reduce interfacial tension and to inhibit droplet coalescence [1–5]. However, environmental concerns, toxicity, and limited stability under harsh conditions have led to the need for alternative stabilizers. Pickering emulsions, which are stabilized by solid particles adsorbed at the liquid/liquid interface, are recognized as a good alternative [6–12]. These emulsions exhibit exceptional stability due to the irreversible adsorption of particles that provide a robust steric and mechanical barrier to droplet coalescence [13–17].

The choice of stabilizing particles plays a key role in the performance of Pickering emulsions, as particle properties directly affect interfacial tension, wettability, and overall emulsion stability [14,16,18]. Inorganic particles, such as silica and clays, have been extensively studied as stabilized in Pickering emulsions [19–24]. However, these materials are not biodegradable and their use has raised toxicological concerns in relation to their

effect in human and environmental health. This has shifted the focus to the use of sustainable materials, such as natural biopolymers and their derivatives [25–27]. In particular, the use of interpolyelectrolyte complexes (IPECs) represents an innovative approach to designing particle-like stabilizers for Pickering emulsions [28,29]. These complexes are formed through electrostatic interactions between oppositely charged polyelectrolytes, with the significant entropy gain associated with the release of counterions into the bulk solution, which accompanies complex formation, being a key factor driving this process. This results in nanoscale or microscale structures with unique interfacial properties. Their tunable composition, charge density, and size make IPECs attractive candidates for emulsion stabilization [30]. It is worth noting that polyelectrolytes alone exhibit very limited surface activity and only induce a measurable change in surface tension at relatively high concentrations, which restricts their utility as stabilizers for emulsions. However, IPECs formed in the aqueous media exhibit particle-like properties, which can be exploited to stabilize emulsions. In fact, these IPECs can adsorb at the water/oil interface as a result of their amphiphilic nature at the oil/water interface. Upon adsorption, the IPECs form an interfacial layer that reduces the interfacial tension, inhibits droplet coalescence, and provides steric and electrostatic stabilization. Additionally, the IPEC layer contributes to the mechanical barrier properties, further enhancing the emulsion stability by preventing the migration and fusion of droplets [28]. This situation is different to that occurring when the complex includes proteins. These present interfacial activity themselves and can contribute to stabilize emulsions before the complexation [31–33].

The seminal work on the stabilization of Pickering emulsions by IPECs was developed by Bago-Rodríguez et al. [28], who employed synthetic polyelectrolytes such as poly(allylamine hydrochloride) and poly(4-styrene sulfonate) sodium salt. They systematically examined the effects of varying the polyelectrolyte mixing ratio, pH, and concentration, revealing that IPECs with compositions near charge neutralization produce the most stable oil-in-water emulsions. Compared to coacervate-stabilized emulsions, IPEC-stabilized emulsions demonstrated superior resistance to coalescence, with increased polyelectrolyte concentrations yielding smaller droplet sizes and improved stability. However, at very high IPEC concentrations, stability decreased due to particle aggregation. This approach was subsequently extended to other synthetic polyelectrolyte pairs, such as poly(diallyldimethylammonium chloride) and anionic polyelectrolyte poly(acrylic acid), further broadening the applicability of IPECs in emulsion stabilization [29]. Sun et al. [34] explored the use of IPECs based on the combination of carboxymethyl-modified tamarind seed polysaccharide and chitosan for the stabilization of Pickering emulsions. They found that IPECs with a 1:1 mass ratio of components exhibited optimal properties, including the smallest particle size, strong interfacial activity, and enhanced emulsifying capacity. Emulsions stabilized by these complexes demonstrated excellent stability and viscoelastic properties, with high internal phase emulsions achievable at very low concentrations. Despite the remarkable potential of IPECs in stabilizing Pickering emulsions, their application remains largely underexplored, particularly when utilizing polyelectrolytes derived from natural sources.

Chitosan (CS) and sodium alginate (ALG) are good candidates for the formation of IPECs [35,36]. CS, a cationic polysaccharide derived from chitin—the second-most abundant polysaccharide in nature—is known for its excellent biocompatibility, antimicrobial activity, and film-forming ability, making it highly versatile for a range of applications. On the other hand, ALG, an anionic polysaccharide derived from seaweed, is valued for its robust gelling properties, biocompatibility, and stability in aqueous environments. The electrostatic interactions between the amine groups of CS and the carboxylate groups of ALG can be exploited to form stable IPECs, which may present interfacial properties ideal

for Pickering emulsion stabilization [37–42]. Therefore, the use of CS and ALG to form IPECs offers several advantages, including their renewable nature, cost-effectiveness, and low toxicity. These aspects are very important due to the growing emphasis on sustainable materials in industrial applications. Additionally, the modular nature of IPECs enables precise control over their physicochemical properties, allowing for the customization of emulsion systems for specific applications.

This work investigates the stabilization of Pickering-type emulsions using CS-ALG IPECs as stabilizers within a water–soybean oil system. Soybean oil was chosen because of its extensive use in food and cosmetic formulations [43–45]. The research focuses on the effect of the charge ratio between CS and ALG-referred to as the compositional ratio or *Z*-ratio-on the preparation and performance of the IPECs on the stabilization of Pickering-like emulsions. In particular, the study investigates how the *Z*-ratio affects the adsorption of IPECs at the water/oil interface and the IPECs' ability to form a robust particle layer at the fluid–fluid interface. In addition, the relationship between IPEC properties and the resulting emulsion properties, including stability, are investigated. Moreover, the role of the volume fractions of liquid phases on the phase behavior of the obtained emulsions will also be explored. The insights gained from this study will contribute to the development of environmentally friendly, stable, and efficient emulsion systems suitable for various practical applications, including food products, pharmaceutical delivery systems, and cosmetic formulations. Furthermore, the inherent tunability of IPEC properties through straightforward modifications presents exciting opportunities for designing responsive or multifunctional emulsions, expanding their potential.

2. Materials and Methods

2.1. Materials

Low molecular weight chitosan (50–190 kDa), with a degree of deacetylation ranging from 75% to 85%, and sodium alginate, with a molecular weight in the range 12–40 kDa, were purchased from Sigma-Aldrich (Darmstadt, Germany). Soybean oil was obtained from Fisher Scientific (Hampton, NH, USA). All chemicals were used as received without further purification. The pH of the aqueous solutions was adjusted using glacial acetic acid (purity $\geq$ 99%) and sodium hydroxide (purity $\geq$ 97%), supplied by Sigma-Aldrich (Darmstadt, Germany) and Fisher Scientific (Hampton, NH, USA), respectively.

The samples were prepared using ultrapure deionized water of Milli-Q quality with a resistivity exceeding 18 MΩ·cm and a total organic carbon content below 6 ppm. This highly pure water was produced using an AquaMAX^{TM}-Ultra 370 Series multicartridge purification system (Young Lin Instrument Co., Ltd., Anyang, Republic of Korea).

2.2. Experimental Methods

All the experiments described in the present work were conducted at a controlled temperature of 25.0 $\pm$ 0.1 °C, and a fixed pH of 4.5. Thus, it was possible to ensure the absence of any influence associated with the environmental conditions between independent experiments.

2.2.1. Preparation of the Dispersions Containing IPECs

The preparation of CS and ALG solutions (pH = 4.5) for the formation of IPECs was performed in accordance with the procedure proposed in our previous studies [46,47]. Briefly, the stock solutions of CS and ALG, with a concentration of 10 g/L, were prepared by weighing the appropriate quantities of CS or ALG and transferring them into a 50 mL flask. The flask was then partially filled with water, followed by the addition of 100 µL of glacial acetic acid to lower the pH. The pH of the resulting solution was carefully adjusted

to 4.5 by dropwise adding a 10^{-2} mM sodium hydroxide solution. Finally, the final volume of the solutions was reached by adding an aqueous solution of glacial acetic acid with its pH fixed at 4.5.

The IPECs were prepared using a mixing method adapted from the original procedure developed by Ravera et al. [48], which was originally established for the preparation of particle–surfactant mixtures. In this approach, equal volumes of the CS and ALG solutions (pH = 4.5) were combined to form the IPEC dispersion. Specifically, a solution of CS at a concentration twice that of the final mixture was added dropwise to a stirred ALG solution at 0.2 g/L (also twice the final target concentration). This stepwise addition was designed to minimize concentration gradients during mixing [49,50]. The resulting dispersions were stirred at 1000 rpm for 30 min to ensure homogeneity and then left undisturbed overnight to allow equilibration. Given that acetic acid does not act as a buffer, pH measurements were conducted both after the ageing period and immediately prior to sample utilization, to ensure stable pH conditions in the vicinity of 4.5. This was also applied to CS and ALG solutions.

2.2.2. Preparation of the Pickering-like Emulsions

Emulsions with a total volume of 10 mL were prepared using a high-speed laboratory mixer ULTRA TURRAX T25 (IKA, Staufen, Germany) operating at 12,000 rpm for 1 min. The emulsions were formulated with varying volume fractions of soybean oil and aqueous dispersions of IPECs. This allows us to define the composition in term of the oil volume fraction as:

$$\phi_o = \frac{V_o}{V_o + V_w}, \tag{1}$$

with V_o and V_w being the volumes of soybean oil and aqueous phase (aqueous dispersion of IPECs) in the emulsion, respectively, and, therefore, the volume fraction of the aqueous phase can be defined as $\phi_w = 1 - \phi_o$.

2.2.3. Characterization of the Dispersions Containing IPECs

The turbidity of the mixtures was determined from absorbance measurements according to the following relationship:

$$\tau = 1 - 10^{-A}, \tag{2}$$

where A represents the absorbance of the sample. The measurements were performed at a wavelength of 450 nm using a Jasco FP-6500 spectrophotometer (Jasco Inc., Tokyo, Japan). This wavelength was selected to prevent interference from adsorption bands of the components.

The effective charge of the complexes was determined by measuring their electrophoretic mobility (u_e) using Laser Doppler Velocimetry with a Zetasizer Nano ZS (Malvern Instruments Ltd., Malvern, UK). The electrophoretic mobility and zeta potential (ζ) can be related through the Henry's equation:

$$u_e = \frac{2\varepsilon}{3\eta}\zeta f(\kappa a), \tag{3}$$

where ε and η represent the dielectric permittivity and the viscosity of the medium, respectively. ζ is the zeta potential and $f(\kappa a)$ is the Henry function, which, in our case, assumes a value of 1.5 as the particle size is larger than the thickness corresponding to the electrical double layer [51].

The apparent hydrodynamic diameter (d_h^{app}) of the IPECs dispersed in water, representing their average size, was determined using dynamic light scattering (DLS). The measurements were conducted using a Zetasizer Nano ZS (Malvern Instruments Ltd.,

Malvern, UK), which was equipped with an He-Ne laser (wavelength 632 nm) operating in a quasi-backscattering configuration (scattering angle of 173°). Prior to measurements, samples were filtered through a 0.45 µm inert filter of cellulose acetate (Fisher Scientific, Hampton, NH, USA) and placed in the measurement cell. The intensity auto-correlation function obtained from DLS experiments was analyzed using the CONTIN method, which allows one to obtain the size distribution of the IPECs. Further details on the DLS methodology and data analysis can be found in previous studies [52,53].

2.2.4. Characterization of the Pickering-like Emulsions Stabilized by IPECs

The characterization of Pickering-like emulsions was performed 2 months after their preparation. This time can be expected to be long enough for emulsions to reach steady state conditions, considering the typical destabilization kinetics of Pickering emulsions [54–57].

The stability of the emulsions was assessed using the average stabilization index (*SI*), defined as the ratio of the volume of the emulsified phase (V_e) to the total volume of the liquid column (V_l). This relationship is expressed as:

$$SI = \frac{V_e}{V_l}. \quad (4)$$

A *SI* value of 0 indicates complete separation into two pure liquid phases, whereas a *SI* of 1 corresponds to 100% emulsification of the liquid column. It is worth noting that the definition of the *SI* is based on the commonly used creaming index [54,58].

To determine the nature of the emulsions obtained, the droplet dispersion test was used. In this test, a drop of the emulsified column is introduced into a large volume of each of the two pure liquids involved in the emulsion. If the liquid phase matches the continuous phase of the emulsion, the drop disperses uniformly without any phase separation. Conversely, if the continuous phase of the emulsion differs in nature from the liquid phase into which it is added, the emulsion droplet exhibits phase separation. A Nikon Eclipse 80i, (Nikon Inc., Minato, Japan) microscope fitted with a CCD camera (model C8800-21C, Hamamatsu Corp., Yokohama, Japan) was used to obtain optical microscopy images of the emulsions.

3. Results

3.1. Assembly of IPECs in Solution

3.1.1. Turbidity Measurements

The first step of this work involved the preparation of IPECs formed by the combination of CS and ALG. These IPECs were later utilized as stabilizers for Pickering-like emulsions. To ensure a comprehensive understanding of their role in emulsion stabilization, the complexes had to be thoroughly characterized, with particular attention to their compositional ratio and physicochemical properties. The IPECs were prepared by varying the compositional Z = cCS/cALG, i.e., the molar ratio of CS amino groups to ALG carboxyl groups, where cCS represents the concentration of deacetylated monomers of CS in the mixture and cALG denotes the concentration of charged monomers of ALG in the mixture. This ratio is a critical parameter for tailoring the properties of the complexes, as it influences the degree of electrostatic association, as well as different physicochemical properties of the obtained IPECs, e.g., particle morphology and overall stability. Figure 1a displays the relationship between the turbidity of the samples and the compositional ratio *Z*.

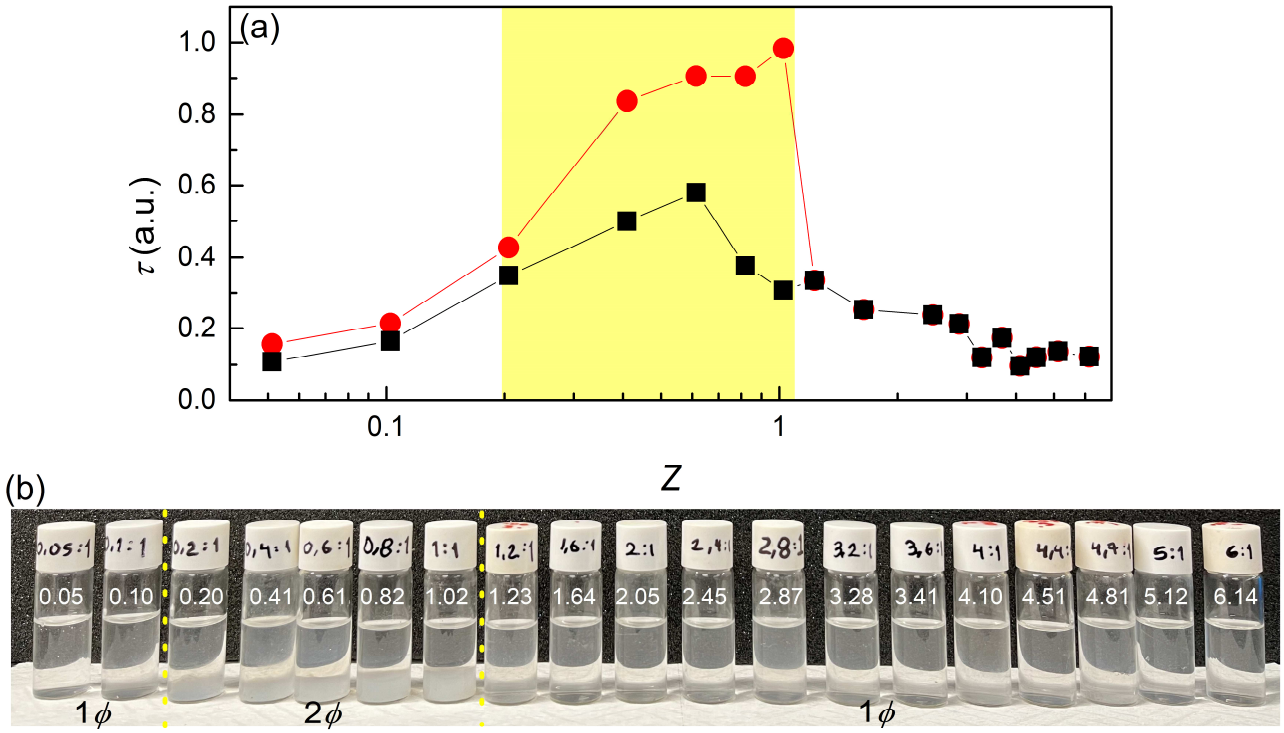

Figure 1. (**a**) Dependence of the turbidity of the mixtures on the compositional ratio *Z*. The figure presents data for freshly prepared samples (■) and samples after 24 h of ageing (●). The lines are visual guides, and the yellow-highlighted region corresponds to the phase separation region. (**b**) Image of a set of samples with different *Z* (indicated in the vial) values after equilibration. The two vertical yellow lines indicate the beginning and end of the phase separation region. The nature of each sample is indicated in the image: 1ϕ corresponds to single-phase systems, and 2ϕ corresponds to biphasic systems.

Turbidity measurements offer valuable insights into the formation and characteristics of IPECs, serving as a direct indicator for the assessment of interactions between constituent biopolymers. In the specific case of the CS-ALG system, the dependency of turbidity on the charge ratio parameter *Z* provides critical information about the extent and nature of complexation, as well as the resulting particle characteristics. Variations in *Z* directly impact the charge balance between CS and ALG, thereby modulating the degree of complexation and the structural attributes of the IPECs. At the lowest *Z* values, where sodium alginate is the dominant component in the mixture, the excess of negatively charged ALG monomers in comparison to the positively charged CS monomers results in the formation of negatively charged complexes. These complexes remain stable in dispersion, forming a single-phase compositional region (1ϕ) characterized by low turbidity. In this region, the turbidity values are so low that the samples appear nearly transparent, as illustrated in Figure 1b. Similarly, at the highest *Z* values, where CS is in excess, stable dispersions are also observed. In this case, the excess of positively charged CS monomers results in the formation of positively charged complexes, which similarly exhibit low turbidity and form a stable 1ϕ region. These findings underscore the stabilizing influence of charge imbalance in these regions, as repulsive interactions between charged complexes are responsible for preventing aggregation. A different behavior was observed in the vicinity of the stoichiometric charge ratio (Z~1). At this point, the charges of CS and ALG are nearly balanced, thereby promoting the formation of charge-compensated complexes. The resulting neutralization diminishes the electrostatic repulsion, thereby facilitating the aggregation or precipitation of the IPECs. This is reflected in a pronounced turbidity peak, which indicates a significant degree of particle aggregation or phase separation. The phase behavior transition to a biphasic system

(2ϕ) is also evidenced by the formation of a dense sediment in the sample containers. The sediment observed for compositions around Z~1 confirmed the transition from a stable dispersion to a phase separated system. It is noteworthy that the phase separation mediated by the aggregation of neutral IPECs, followed by the sedimentation of the resulting aggregates, is clearly evidenced by the temporal evolution of the turbidity peak. In particular, the turbidity of samples with compositions within the phase separation region decreased over a period of 24 h. This reduction in turbidity is consistent with the sedimentation of IPEC aggregates, as turbidity measurements evaluate the optical properties of the liquid phase, i.e., the supernatant in phase-separated mixtures. This phenomenon is corroborated by observations in Figure 1b, where sedimentation is visually apparent, further confirming the biphasic nature of these samples. The above discussed evolution of turbidity with the ageing of the IPECs and the Z-ratio is not new. In fact, similar behaviors have been observed in mixtures of oppositely charged polyelectrolyte [59], but also in oppositely charged polyelectrolyte–surfactant mixtures [49,60].

3.1.2. ζ-Potential Measurements

The ζ-potential of the samples was analyzed to gain a better understanding of the association process in the formation of IPECs. This parameter provides a quantitative measure of the charge density at the slipping plane that can be considered proportional to the effective charge of the IPECs and its sign, giving insight into the surface charge characteristics of the IPECs formed in solution. The ζ potential is particularly valuable for assessing the extent of charge compensation and the stability of the complexes in different compositional regimes. Figure 2 shows the dependence of the ζ potential on the Z-ratio for the oppositely charged polyelectrolyte mixtures investigated in this study.

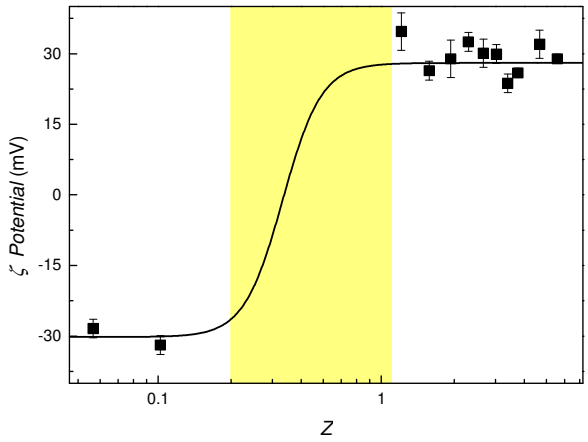

Figure 2. Dependence of the ζ-potential of IPECs on the Z-ratio. Note that only single-phase samples can be evaluated by electrophoretic mobility measurements for the determination of the ζ-potential. The line is a guide for the eyes and the yellow shaded area corresponds to the phase separation region.

The electrophoretic mobility measurements are in close agreement with the findings from turbidity analysis, thus providing a coherent picture of the system's behavior. Two different compositional regions were identified in which charged interpolyelectrolyte IPECs were formed. These regions overlap with the samples exhibiting low turbidity values, which indicates the formation of stable complexes. This can be understood by considering that the effective charge of the complexes is governed by the polysaccharide with the higher molar fraction in the mixtures, as may be expected for a complexation driven by electrostatic interactions. Therefore, when the value of Z is less than one, the complexes exhibit an excess of sodium alginate monomers, which results in a negative net

charge for the IPECs. Conversely, for Z values greater than one, the molar fraction of CS in the IPECs is higher than that of ALG, leading to a charge inversion phenomenon, whereby the IPECs display a positive charge. The transitional zone between these two regions is characterized by unstable complexes, with an effective charge that approaches zero. This instability region is characterized by high turbidity values, which indicate significant heterogeneity and potential aggregation within the system. This transition reflects the progressive neutralization and inversion of charge as the result of the complexation between the polyelectrolytes, thereby highlighting the critical role of Z in determining the stability and charge characteristics of the complexes as occurs in oppositely charged polyelectrolyte–surfactant mixtures [49], but also in the assembly of polyelectrolyte layers on charged liposomes as shown by Ruano et al. [61].

3.1.3. Dynamic Light Scattering Measurements

Dynamic light scattering (DLS) measurements were carried out to gain further insight into the properties of the IPECs as particle-like materials for stabilizing Pickering emulsions. These measurements provide information on the average size and polydispersity of the aggregates formed in the aqueous medium, expressed in terms of the distribution of apparent hydrodynamic diameters. Figure 3 shows a set of intensity autocorrelation functions ($g^{(2)}(t) - 1$) and the apparent hydrodynamic diameter distributions obtained from their analysis.

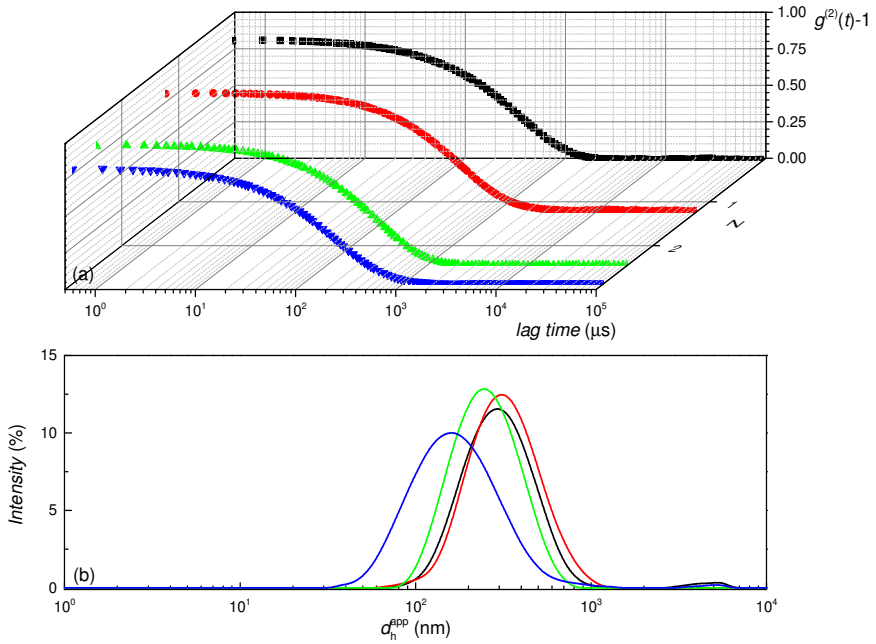

Figure 3. DLS results: intensity autocorrelation function for aqueous dispersions of IPECs with different values of Z (**a**) and apparent hydrodynamic diameter distribution obtained from the analysis of the intensity autocorrelation functions (**b**). In both panels the color code is the same: (—) Z = 0.05, (—) Z = 1.23, (—) Z = 2.45, and (—) Z = 2.87.

The analysis of the intensity autocorrelation functions reveals a monotonic, exponential-like decay over time, characterized by a single distribution of relaxation times. This suggests that the IPECs in the aqueous medium display relatively simple monomodal dynamics, which indicates the formation of particles with a wide but single-size distribution. Furthermore, the data reveal a shift to smaller characteristic decay times in the intensity autocorrelation functions as the Z-ratio increases, suggesting a decrease in the size of the complexes. On the other hand, as the composition separates from the boundaries of the phase separation region, the intensity autocorrelation functions undergo a displacement to

lower values of the characteristic relaxation time, which is a signature of the decrease in the size of the IPECs. This is confirmed by the apparent hydrodynamic diameter distributions displayed in Figure 3b. In addition to the above discussion, the apparent hydrodynamic diameter distributions show that even though the formed IPECs present a single population, it is relatively broad, indicating complexes with a high polydispersity.

A clearer understanding of the characteristic dimensions of the formed IPECs can be obtained from the analysis of the average apparent hydrodynamic diameter. For this purpose, Figure 4 shows the dependence of the average apparent hydrodynamic diameter of the IPECs on the *Z* value for CS-ALG complexes.

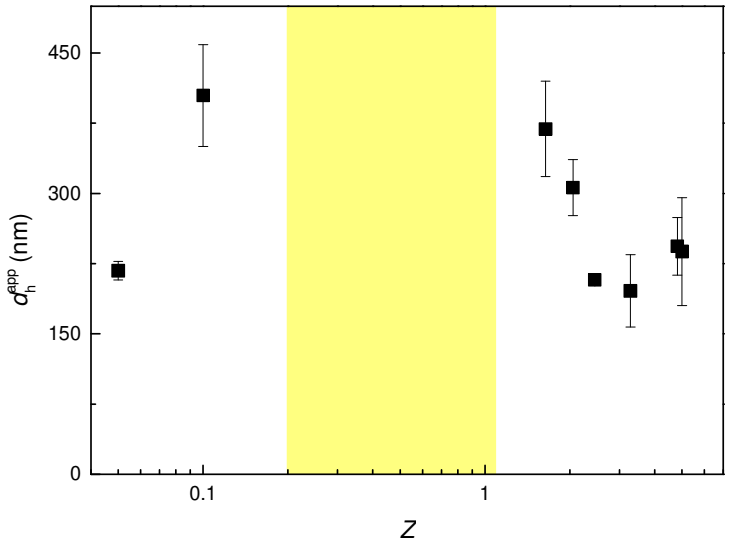

Figure 4. Dependence of the average apparent hydrodynamic diameter of IPECs on the *Z*-ratio. The yellow shaded area corresponds to the phase separation region. The error bars indicate the standard deviation between the average values of the 5 independent measurements obtained for each sample.

The results indicate that the IPECs in solution tend to increase in size as the *Z* value approaches the phase separation region. This behavior is important for the formation of Pickering emulsions as particle size and colloidal stability are key parameters influencing their effectiveness as stabilizers. At *Z* values close to the phase separation region, the complexes experience conditions of low colloidal stability, favoring the formation of larger aggregates which eventually sediment as a solid phase for *Z* about 1. Conversely, for compositions far from $Z = 1$, the size of the aggregates decreases and reaches a stable value of around 200 nm, regardless of the mixture composition. The smaller, more stable particles may be particularly important for the formation of stable emulsions as their size is in the optimal range for adsorption at oil/water interfaces. It is important to note that a direct comparison of the IPEC sizes obtained in this study with those reported in the literature is not possible, as there is no consensus on the relationship between complex composition and aggregate size [28]. This highlights the need for systematic studies to establish size–composition correlations, particularly for applications in Pickering emulsions.

3.2. Phase Diagram of Pickering-like Emulsions Stabilized by IPECs

The previous sections focused on the examination of the understanding of the electrostatic association between CS and ALG in aqueous solution, resulting in the formation of interpolyelectrolyte complexes. These complexes exhibit a surface charge and, consequently, a degree of affinity for the aqueous medium that can be modulated in terms of the compositional ratio (*Z*-ratio), that is, by the mole fraction of the components in the mixture. It may, therefore, be assumed that by modifying *Z*, it will be possible to tune the

complexes' affinity for the water/oil interfaces, including the water/soybean oil interface, which will consequently affect their capacity to stabilize emulsions. The stabilization of emulsions with these complexes may be considered analogous to the stabilization of Pickering emulsions with solid colloidal particles. It is noteworthy that the ability of both CS and ALG to stabilize emulsions in the system studied is negligible, with phase separation occurring almost immediately after preparation. This indicates that the surface activity of the chosen polymers pair is very limited at the soybean oil/water interface. However, when complexation occurs, for specific compositions, IPECs formation may be exploited to stabilize emulsions. Figure 5 shows the appearance of the water/oil/biopolymer ternary mixtures for specific compositions after the homogenization process.

Figure 5. Set of images for emulsions stabilized by IPECs with different values of the *Z*-ratio (indicated in the images) and different volume fractions of the liquid phases (**a**) ϕ_o = 0.10, (**b**) ϕ_o = 0.75, and (**c**) ϕ_o = 0.90. Images correspond to emulsions aged for 2 months.

It is noteworthy that, in the case of mixtures with *Z* values close to one, an optimal emulsification capacity might be expected due to the neutrality of the complexes formed, which would favor their depletion from the aqueous phase. However, due to the instability of these complexes, it is not possible to study emulsions using mixtures with compositions close to phase separation. The images provide valuable insights; firstly, they reveal the absence of transitional phase inversion, i.e., a phase inversion driven by changes in the concentration of the stabilizing agent or, in this case, by variations in the *Z*-ratio [62]. This indicates that for the *Z* values at which emulsions form, given a constant value of ϕ_o, the nature of the emulsion remains independent on the value of *Z*. The absence of transitional phase inversion suggests that the amphiphilic balance of the IPECs remains relatively constant across the studied *Z*-ratios, favoring stabilization of the dispersed phase without abrupt changes in interfacial affinity. On the other hand, the emulsions form in the minority phase, that is, in the region corresponding to the phase that is in the lower proportion

in the system. This suggests that the formation of emulsions involves the dispersion of droplets of the phase with higher volume fraction within the phase with lower volume fraction. The excess of the phase that cannot be dispersed as droplets appears as a creamed or sedimented liquid column, depending on the density differences between the phases involved. It is also important to note that the images evidence an increase in the size of the emulsified column as Z increases, which is an indication of the reduction of the importance of the destabilization phenomena. Furthermore, it is worth analyzing the effect of the ratio between the volume fractions of the liquid phases at fixed Z values. Figure 6 presents four series of emulsions prepared at constant Z values but with varying volume fractions of the oil phase.

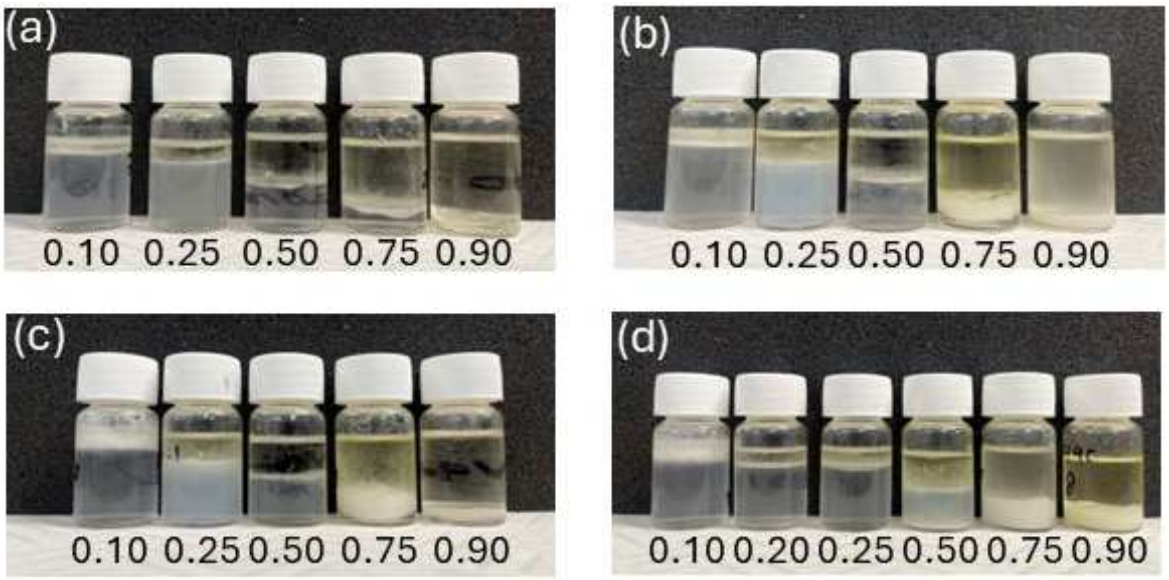

Figure 6. Set of images for emulsions stabilized by IPECs with fixed value of the Z-ratio and different volume fractions of the liquid phases (indicated in the images). (**a**) Z = 1.23, (**b**) Z = 2.45, and (**c**) Z = 3.28. (**d**) Z = 5.12. Images correspond to emulsions aged for 2 months.

The results indicate that emulsion formation and its characteristics vary depending on both the value of Z and ϕ_o. The images reveal that, at low Z values, emulsions do not form regardless of the value of ϕ_o. As the Z value increases, emulsions begin to form when ϕ_o is small. A further increase in Z leads to the formation of emulsions with different characteristics compared to those observed at low ϕ_o values, particularly at higher ϕ_o values. However, emulsions do not form for intermediate values of the oil phase volume fraction. This behavior suggests the existence of a catastrophic phase inversion driven by the ratio between the volume fractions of the liquid phases.

To identify the nature of the emulsions obtained, the droplet dispersion test was employed. Figure 7 illustrates an example of the results obtained from this test, which provide insights into the characteristics of the emulsions studied. In Figure 7a, the addition of an emulsion droplet to water results in the appearance of a cream layer at the top of the liquid. Conversely, in Figure 7b, the emulsion droplet completely disperses in the vial containing soybean oil. This indicates that the emulsion in question has a water-in-oil (W/O) character, as adding it to water causes creaming at the top of the liquid. Following the same approach, the addition of an oil-in-water (O/W) emulsion droplet to a vial containing water would result in dispersion, forming a homogeneous liquid phase. On the contrary, adding the same O/W emulsion to a vial containing soybean oil led to sedimentation of the water-rich droplet at the bottom of the liquid phase. This behavior is observed in Figure 7c,d, respectively.

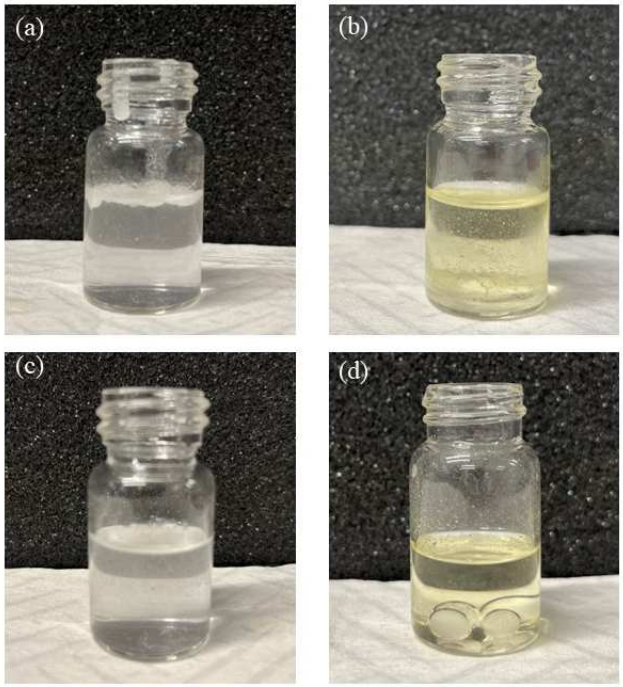

Figure 7. Images obtained from the test for the determination of the type of emulsion obtained. (**a**) Dispersion of a drop of W/O emulsion in water. (**b**) Dispersion of a drop of W/O emulsion in soybean oil. (**c**) Dispersion of a drop of O/W emulsion in water. (**d**) Dispersion of a drop of O/W emulsion in soybean oil. Images correspond to emulsions aged for 2 months.

From the above observations, it can be inferred that O/W emulsions tend to form at the top of the liquid column. Conversely, W/O emulsions tend to form at the bottom of the liquid column. Based on the analysis of the nature of the different types of emulsions, a compositional map for the system was developed, as shown in Figure 8. This map illustrates the narrow compositional range in which Pickering emulsions stabilized by IPECs (formed from CS and ALG) can form at pH = 4.5.

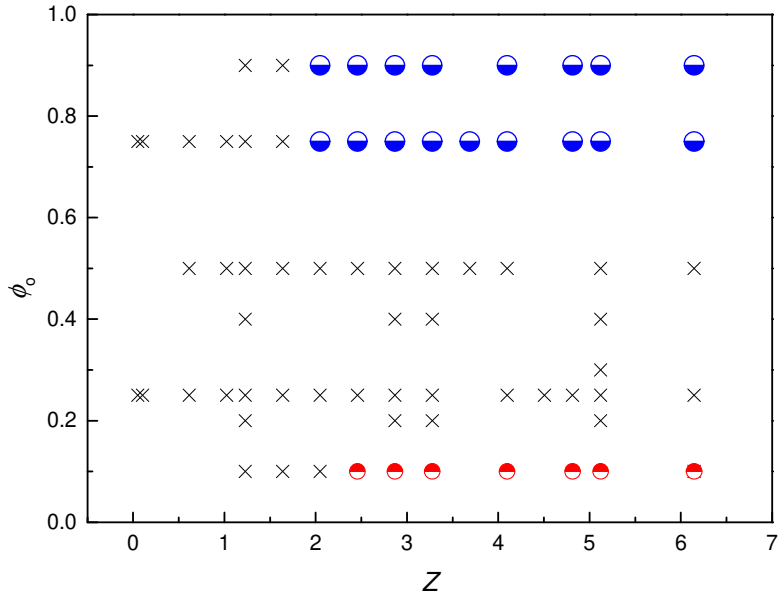

Figure 8. Compositional map ϕ_o-Z for two-phase systems formed by aqueous dissolution of IPECs and soybean oil. The diagram shows the different types of systems obtained with different symbols: (×) Phase-separated systems, (◒) W/O emulsions and (◓) O/W emulsions. Results correspond to emulsions aged for 2 months.

The analysis of the compositional map reveals that, in systems where water is the main component (ϕ_o = 0.10), O/W emulsions form when $Z > 2$. On the other hand, in systems where the oil phase is dominant ($\phi_o \geq 0.75$), W/O emulsions form when $Z \geq 2$. For other compositions, emulsion formation was not observed. Interestingly, for a fixed Z value, as ϕ_o increases, a transition was observed from O/W emulsions to W/O emulsions through a phase separation region. Several studies have reported that phase inversion, particularly catastrophic phase inversion, can occur due to changes in the volume fractions of the liquid phases [63,64]. In the case of O/W emulsions, increasing the oil volume fraction drives the system toward the formation of a W/O emulsion. This transition occurs as the coalescence of oil-phase droplets leads to the reorganization of the continuous phase, with water forming discrete droplets. Typically, this type of phase inversion is manifested as a sharp transition, where phase inversion occurs through a state where the entire liquid column is fully emulsified [63], at a specific ratio between the volume fractions of the two liquid phases. However, unlike systems stabilized by solid particles, in this study, the catastrophic phase inversion of emulsions stabilized by IPECs does not appear as a sharp transition. Instead, a region is observed where complete phase separation occurs between the compositional domains corresponding to O/W and W/O emulsions. This behavior can be explained by considering the role of IPECs in stabilizing emulsions. As the ϕ_o increases, the number of IPECs available in the water/oil system decreases. Thus, once ϕ_o exceeds a threshold value, the concentration of IPECs may become insufficient to form a dense interfacial film at the water/oil interface, leading to emulsion destabilization and phase separation. At higher values of ϕ_o, despite the reduced availability of IPECs, the volume fraction of the minority phase (water) is also significantly reduced. Under these conditions, the available IPECs may be sufficient to stabilize the water/oil interface, preventing coalescence and resulting in the formation of W/O emulsions. It is worth noting that the change in the hydrophilic–lipophilic balance (HLB) of the IPECs may alter the phase inversion pattern. This may be especially important under extreme conditions, i.e., highly hydrophilic or hydrophobic IPECs. However, within the compositional region explored in this study, there is no evidence of modification in the capacity of the IPECs to stabilize O/W or W/O emulsions with the modification of Z.

3.3. Stability of IPECs Pickering-like Emulsions

The above results have pointed out that IPECs can act as emulsifying agents under specific conditions. These emulsions can undergo either creaming or sedimentation processes depending on their nature. The stability of the emulsions can be assessed using the stabilization index (*SI*), which measures the volumetric fraction of the emulsion relative to the total volume of the liquid column. Figure 9 shows the dependence of *SI* on the Z-ratio for emulsions with varying ϕ_o values.

For conditions where stable emulsions were obtained after 2 months of ageing, the stability index (*SI*)—and hence emulsion stability—tends to increase with increasing Z. At first glance, it may seem counter-intuitive, since an increase in Z (beyond Z = 1) increases the charge on the complexes, and hence their solubility in the continuous phase, potentially destabilizing the emulsion. However, this increase in Z also increases the concentration of CS available for complexation, and, given the amphiphilic nature of CS characterized by a molar fraction of acetylated monomer of approximately 15–25%, higher CS concentrations increase the availability of amphiphilic residues. These amphiphilic residues can preferentially adsorb at the water/oil interface where they help to reduce the interfacial tension and stabilize the emulsion. This dual behavior—increased solubility coupled with enhanced interfacial activity—highlights the critical role of Z in modulating emulsion properties. On the other hand, the stability of W/O emulsions increases as ϕ_o approaches the limit

where emulsions cease to form. This trend is similar to the behavior observed in Pickering emulsions stabilized with conventional particles, where stability increases near the phase inversion region [62,63,65–67]. This phenomenon can be explained by considering the interplay between interfacial adsorption and the volume fraction of the dispersed phase. For a fixed number of particles, decreasing the volume fraction of the dispersed phase leads to the formation of a denser interfacial layer of complexes of fixed composition around the droplets. This denser interfacial structure is likely to increase resistance to coalescence and improve overall emulsion stability. These findings highlight the complex interplay between composition, interfacial activity, and phase fraction in determining the stability of emulsions.

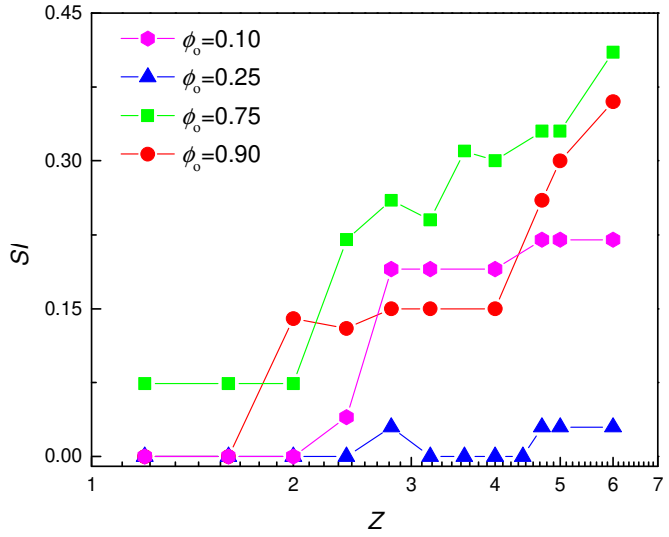

Figure 9. Dependence of the stabilization index, *SI*, on the value of the *Z*-ratio for emulsions with different volume fractions of liquid phases. Note that the emulsions obtained for ϕ_o = 0.10 are of W/O type while the emulsions obtained for ϕ_o = 0.75 and 0.90 are of O/W type, while for ϕ_o = 0.25 no emulsion was obtained as shown by the values of *SI* close to 0. Results correspond to emulsions aged for 2 months.

3.4. Morphological Characterization of Pickering-like Emulsions

Microscopic characterization may provide insights into droplet morphology and size. Figure 10 presents optical microscopy images of emulsions prepared by varying ϕ_o and the *Z*-ratio of the IPECs used for stabilization.

A general observation is that the density of emulsions increases as the *Z*-ratio increases, which is consistent with the increased stability of emulsions under these conditions. This trend is particularly evident in emulsions with a value of *Z* where a bigger number of droplets or denser emulsion films can be observed in the images. The increase in the number of emulsion droplets is a signature of reduced coalescence and/or reduced Ostwald ripening tendencies. These results emphasize the role of the compositional ratio, not only in promoting stability, but also in influencing emulsion microstructure.

For O/W emulsions formed at low ϕ_o values, the droplets exhibit high polydispersity with sizes ranging from a few microns to tens of microns, with most of the droplets having a diameter in the range 20–30 μm. As *Z* increases, the droplet size distribution becomes narrow, the polydispersity decreases, and the droplets assume a diameter of around 20–30 μm. This can be ascribed to the reduction on the average size of the particles that allows the formation of denser interfacial layers as occurs for colloidal particles, preventing coalescence and Ostwald ripening [68]. At low *Z* values, the stabilization provided by the complexes is insufficient, leading to a tendency of the system to reduce the interfacial area. This promotes droplet coalescence and, ultimately, phase separation due to insufficient

coverage and stabilization of the water/oil interface. On the contrary, the narrowing of the size distribution at higher *Z*-ratios indicates improved interfacial coverage and stabilization efficiency, suppressing destabilizing mechanisms such as coalescence. In contrast, for W/O emulsions formed at high ϕ_o values, a distinct transition is observed as ϕ_o increases. At the lower values of ϕ_o for which emulsion formation is possible, discrete water droplets are stabilized within the oil phase. However, as ϕ_o increases, the system undergoes a transition to a bicontinuous emulsion structure [69–71]. This structure, often referred to as a bicontinuous interfacially jammed emulsion gel (bijel), results from the gelation of the interfacial layer. In this state, the system forms a continuous water network within the oil phase, with the stabilizing complexes forming a highly structured, interfacially jammed network. This transition reflects the preference of the system to minimize free energy by forming a less thermodynamically unstable structure.

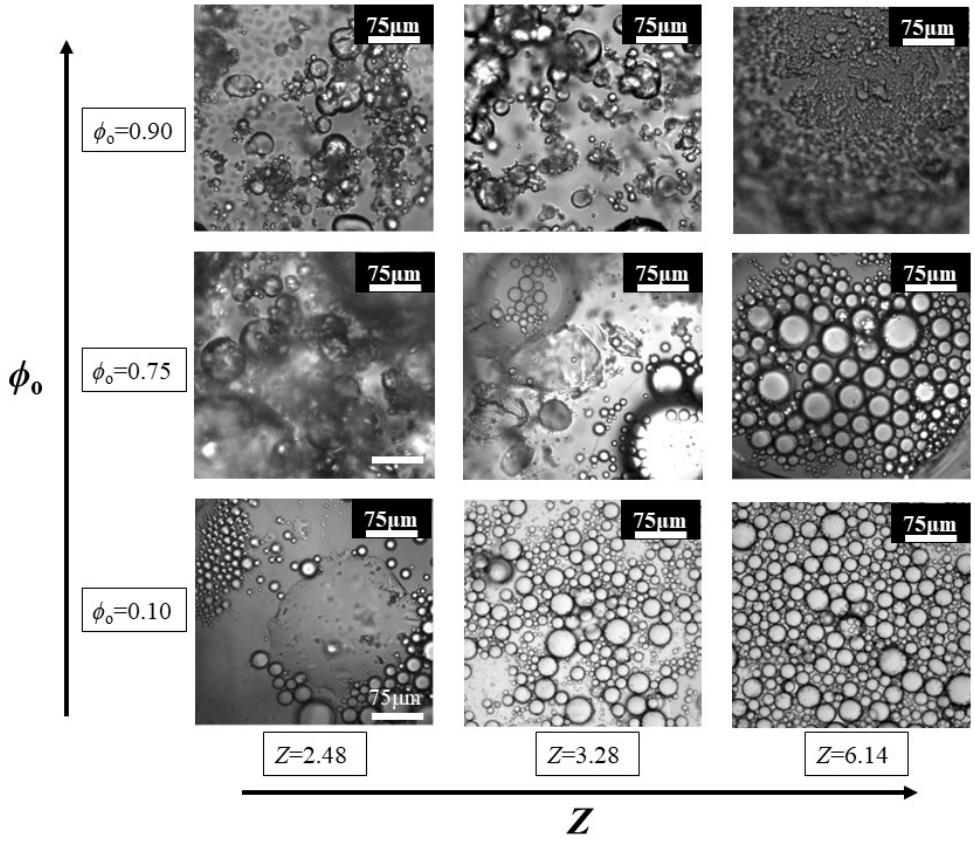

Figure 10. Optical microscopy images for emulsions prepared by varying the volume fraction of the oil phase and the *Z*-ratio of the IPECs used for their stabilization. Images correspond to emulsions aged for 2 months.

4. Conclusions

The stabilization of Pickering-like emulsions using bio-based IPECs composed of CS and ALG represents a transformative approach to designing sustainable and effective emulsifying systems. The findings of this study underscore the critical role of the compositional ratio (Z) and oil volume fraction (ϕ_o) in determining the physicochemical properties, stability, and morphology of the emulsions. The *Z*-ratio, which governs the relative concentrations of CS amino groups and ALG carboxyl groups, was shown to modulate the stability of the complexes, with stable single-phase IPECs forming when the *Z*-ratios were either below or above the stoichiometric balance (*Z*~1). Far from this boundary, charge imbalance prevents aggregation, whereas near *Z*~1, charge neutrality leads to aggregation, resulting in

phase-separated systems. This highlights the importance of precise compositional control in designing effective stabilizers.

Emulsion stability was found to improve significantly with increasing Z, which may be ascribed to an enhanced interfacial activity of the IPECs, associated with the amphiphilic character of CS, playing a crucial role in stabilizing emulsions by preferentially adsorbing at the oil/water interface. Therefore, the dual functionality—reducing interfacial tension while forming robust interfacial layers—leads to reduced coalescence and Ostwald ripening. The phase diagram analysis revealed well-defined regions of O/W and W/O emulsions, demonstrating the tunability of these systems. At low ϕ_o, O/W emulsions are formed, with lower polydispersity as Z increases, reflecting improved stabilization. On the other hand, at high $\phi_{o,}$ W/O emulsions are formed and undergo a transition to bicontinuous interfacially jammed emulsion gels (bijels) as ϕ_o increases. This transition is significant as bijels offer unique structural properties with potential applications in advanced material design, such as templating porous materials or delivering active agents.

These insights highlight the versatility of CS-ALG IPECs as eco-friendly stabilizers. Their biodegradability, biocompatibility, and renewable origin make them particularly suitable for applications in food, cosmetics, and pharmaceuticals, aligning with the increasing demand for sustainable materials. Furthermore, the modularity of IPECs allows for the fine-tuning of their properties to achieve specific stability and performance requirements. For instance, modifying the degree of acetylation in CS or the molecular weight of the components could enable precise control over emulsion characteristics, expanding their applicability to customized formulations.

Future research could explore how IPECs influence interfacial properties and emulsion behavior across a wider range of conditions. Investigations into scalable production methods for CS-ALG IPECs would also be critical to ensure their industrial viability while retaining their eco-friendly advantages. Application-specific optimizations, such as tailoring emulsions for active compound delivery or enhancing stability in food, pharmaceutical, or cosmetic formulations, may expand the use cases of these systems. Moreover, evaluating the long-term stability of these emulsions under varying storage conditions, including temperature and ionic strength, would provide valuable insights for real-world applications. Finally, assessing the environmental impact and lifecycle of these bio-based systems would help solidify their position as sustainable alternatives to synthetic stabilizers.

In summary, the unique properties of these bio-based complexes, coupled with their adaptability, place them as a promising alternative to synthetic stabilizers, advancing the field of colloidal and interfacial science toward a more sustainable future.

Author Contributions: Conceptualization, E.G.; methodology, F.J.G.-V. and E.G.; software, F.J.G.-V. and E.G.; validation, E.G.; formal analysis, F.J.G.-V. and E.G.; investigation, F.J.G.-V., F.O., R.G.R. and E.G.; resources, F.O. and R.G.R.; data curation, E.G.; writing—original draft preparation, E.G.; writing—review and editing, F.O. and R.G.R.; visualization, E.G.; supervision, R.G.R. and E.G.; project administration, F.O. and R.G.R.; funding acquisition, F.O., R.G.R. and E.G. All authors have read and agreed to the published version of the manuscript.

Funding: The work was supported under the grant PID2023-147156NB-I00 funded by MCIN/AEI/10.13039/501100011033 (Spain), the grant PR12/24-31566 (Ayudas para la Financiación de Proyectos de Investigación UCM 2023), and the European Innovative Training Network-Marie Sklodowska-Curie Action NanoPaInt (grant agreement 955612), funded by the E.U.

Data Availability Statement: Data are available upon request.

Acknowledgments: The authors express their gratitude to the Unidad de Espectroscopía y Correlación (CAI de Técnicas Químicas) at Universidad Complutense de Madrid for granting access to their facilities.

Conflicts of Interest: The authors declare no conflicts of interest. The funders had no role in the design of the study; in the collection, analyses, or interpretation of data; in the writing of the manuscript; or in the decision to publish the results.

References

1. Lee, J.; Babadagli, T. Comprehensive Review on Heavy-Oil Emulsions: Colloid Science and Practical Applications. *Chem. Eng. Sci.* **2020**, *228*, 115962. [CrossRef]
2. Bai, L.; Huan, S.; Rojas, O.J.; McClements, D.J. Recent Innovations in Emulsion Science and Technology for Food Applications. *J. Agric. Food Chem.* **2021**, *69*, 8944–8963. [CrossRef] [PubMed]
3. Wang, C.; Zhang, Z.; Wang, Q.; Wang, J.; Shang, L. Aqueous Two-Phase Emulsions toward Biologically Relevant Applications. *Trends Chem.* **2023**, *5*, 61–75. [CrossRef]
4. Israelachvili, J. The Science and Applications of Emulsions—An Overview. *Colloids Surf. A* **1994**, *91*, 1–8. [CrossRef]
5. Lucia, A.; Guzmán, E. Emulsions Containing Essential Oils, Their Components or Volatile Semiochemicals as Promising Tools for Insect Pest and Pathogen Management. *Adv. Colloid Interface Sci.* **2021**, *287*, 102330. [CrossRef] [PubMed]
6. Guzmán, E.; Ortega, F.; Rubio, R.G. Pickering Emulsions: A Novel Tool for Cosmetic Formulators. *Cosmetics* **2022**, *9*, 68. [CrossRef]
7. Venkataramani, D.; Tsulaia, A.; Amin, S. Fundamentals and Applications of Particle Stabilized Emulsions in Cosmetic Formulations. *Adv. Colloid Interface Sci.* **2020**, *283*, 102234. [CrossRef]
8. Yan, X.; Ma, C.; Cui, F.; McClements, D.J.; Liu, X.; Liu, F. Protein-Stabilized Pickering Emulsions: Formation, Stability, Properties, and Applications in Foods. *Trends Food Sci. Technol.* **2020**, *103*, 293–303. [CrossRef]
9. Pickering, S.U. CXCVI.—Emulsions. *J. Chem. Soc. Trans.* **1907**, *91*, 2001–2021. [CrossRef]
10. Ramsden, W. Separation of Solids in the Surface-Layers of Solutions and 'Suspensions' (Observations on Surface-Membranes, Bubbles, Emulsions, and Mechanical Coagulation).—Preliminary Account. *Proc. Roy. Soc. Lond.* **1904**, *72*, 156–164. [CrossRef]
11. Guzmán, E. Pickering Emulsions in Catalytic Processes. *ChemCatChem* **2024**, *16*, e202400856. [CrossRef]
12. Rodriguez, A.M.B.; Binks, B.P. Catalysis in Pickering Emulsions. *Soft Matter* **2020**, *16*, 10221–10243. [CrossRef]
13. de Carvalho-Guimarães, F.B.; Correa, K.L.; de Souza, T.P.; Rodríguez Amado, J.R.; Ribeiro-Costa, R.M.; Silva-Júnior, J.O.C. A Review of Pickering Emulsions: Perspectives and Applications. *Pharmaceuticals* **2022**, *15*, 1413. [CrossRef] [PubMed]
14. Sun, Z.; Yan, X.; Xiao, Y.; Hu, L.; Eggersdorfer, M.; Chen, D.; Yang, Z.; Weitz, D.A. Pickering Emulsions Stabilized by Colloidal Surfactants: Role of Solid Particles. *Particuology* **2022**, *64*, 153–163. [CrossRef]
15. Binks, B.P. Colloidal Particles at a Range of Fluid–Fluid Interfaces. *Langmuir* **2017**, *33*, 6947–6963. [CrossRef]
16. Guzmán, E.; Martínez-Pedrero, F.; Calero, C.; Maestro, A.; Ortega, F.; Rubio, R.G. A Broad Perspective to Particle-Laden Fluid Interfaces Systems: From Chemically Homogeneous Particles to Active Colloids. *Adv. Colloid Interface Sci.* **2022**, *302*, 102620. [CrossRef] [PubMed]
17. Maestro, A.; Guzmán, E.; Ortega, F.; Rubio, R.G. Contact Angle of Micro- and Nanoparticles at Fluid Interfaces. *Curr. Opin. Colloid Interface Sci.* **2014**, *19*, 355–367. [CrossRef]
18. Maestro, A. Tailoring the Interfacial Assembly of Colloidal Particles by Engineering the Mechanical Properties of the Interface. *Curr. Opin. Colloid Interface Sci.* **2019**, *39*, 232–250. [CrossRef]
19. Liu, L.; Pu, X.; Tao, H.; Chen, K.; Guo, W.; Luo, D.; Ren, Z. Pickering Emulsion Stabilized by Organoclay and Intermediately Hydrophobic Nanosilica for High-Temperature Conditions. *Colloids Surf. A* **2021**, *610*, 125694. [CrossRef]
20. Lisuzzo, L.; Cavallaro, G.; Milioto, S.; Lazzara, G. Pickering Emulsions Stabilized by Halloysite Nanotubes: From General Aspects to Technological Applications. *Adv. Mater. Interfaces* **2022**, *9*, 2102346. [CrossRef]
21. Lu, T.; Gou, H.; Rao, H.; Zhao, G. Recent Progress in Nanoclay-Based Pickering Emulsion and Applications. *J. Environ. Chem. Eng.* **2021**, *9*, 105941. [CrossRef]
22. Kumar, G.; Mani, E.; Sangwai, J.S. Impact of Surface-Modified Silica Nanoparticle and Surfactant on the Stability and Rheology of Oil-in-Water Pickering and Surfactant-Stabilized Emulsions under High-Pressure and High-Temperature. *J. Mol. Liq.* **2023**, *379*, 121620. [CrossRef]
23. Heidari, F.; Jafari, S.M.; Ziaiifar, A.M.; Anton, N. Preparation of Pickering Emulsions Stabilized by Modified Silica Nanoparticles via the Taguchi Approach. *Pharmaceutics* **2022**, *14*, 1561. [CrossRef] [PubMed]
24. Zhang, L.; Zhang, G.; Ge, J.; Jiang, P.; Ding, L. PH- and Thermo-Responsive Pickering Emulsion Stabilized by Silica Nanoparticles and Conventional Nonionic Copolymer Surfactants. *J. Colloid Interface Sci.* **2022**, *616*, 129–140. [CrossRef]
25. Zhao, Q.; Fan, L.; Li, J. Biopolymer-Based Pickering High Internal Phase Emulsions: Intrinsic Composition of Matrix Components, Fundamental Characteristics and Perspective. *Food Res. Int.* **2023**, *165*, 112458. [CrossRef] [PubMed]
26. Ribeiro, E.F.; Morell, P.; Nicoletti, V.R.; Quiles, A.; Hernando, I. Protein- and Polysaccharide-Based Particles Used for Pickering Emulsion Stabilisation. *Food Hydrocoll.* **2021**, *119*, 106839. [CrossRef]
27. Zhao, Q.; Fan, L.; Li, J.; Zhong, S. Pickering Emulsions Stabilized by Biopolymer-Based Nanoparticles or Hybrid Particles for the Development of Food Packaging Films: A Review. *Food Hydrocoll.* **2024**, *146*, 109185. [CrossRef]

28. Bago Rodriguez, A.M.; Binks, B.P.; Sekine, T. Novel Stabilisation of Emulsions by Soft Particles: Polyelectrolyte Complexes. *Faraday Discuss.* **2016**, *191*, 255–285. [CrossRef] [PubMed]
29. Bago Rodriguez, A.M.; Binks, B.P.; Sekine, T. Emulsion Stabilisation by Complexes of Oppositely Charged Synthetic Polyelectrolytes. *Soft Matter* **2018**, *14*, 239–254. [CrossRef] [PubMed]
30. Fay, J.M.; Kabanov, A.V. Interpolyelectrolyte Complexes as an Emerging Technology for Pharmaceutical Delivery of Polypeptides. *Rev. Adv. Chem.* **2022**, *12*, 137–162. [CrossRef]
31. Zinoviadou, K.G.; Scholten, E.; Moschakis, T.; Biliaderis, C.G. Properties of Emulsions Stabilised by Sodium Caseinate–Chitosan Complexes. *Int. Dairy J.* **2012**, *26*, 94–101. [CrossRef]
32. Stone, A.K.; Nickerson, M.T. Formation and Functionality of Whey Protein Isolate–(Kappa-, Iota-, and Lambda-Type) Carrageenan Electrostatic Complexes. *Food Hydrocoll.* **2012**, *27*, 271–277. [CrossRef]
33. Jourdain, L.; Leser, M.E.; Schmitt, C.; Michel, M.; Dickinson, E. Stability of Emulsions Containing Sodium Caseinate and Dextran Sulfate: Relationship to Complexation in Solution. *Food Hydrocoll.* **2008**, *22*, 647–659. [CrossRef]
34. Sun, F.; Pan, C.; Liu, Y.; Yang, N. Carboxymethyl Tamarind Seed Polysaccharide/Chitosan Complexes through Electrostatic Interaction Stabilize High Internal Phase Emulsions: Roles of the Mass Ratio and Oil-Water Interfacial Activity. *LWT* **2024**, *195*, 115833. [CrossRef]
35. Torlopov, M.A.; Vaseneva, I.N.; Mikhaylov, V.I.; Martakov, I.S.; Legki, P.V.; Sitnikov, P.A. Chitin Nanocrystals/Alginate Complex for Tuning Stability, Rheology and Bioavailability of Cholecalciferol in Pickering Emulsions. *Int. J. Biol. Macromol.* **2024**, *264*, 130671. [CrossRef] [PubMed]
36. Gu, C.-Y.; Shao, J.-Q.; Liu, X.-L.; Wei, J.-T.; Huang, G.-Q.; Xiao, J.-X. Spray Drying the Pickering Emulsions Stabilized by Chitosan/Ovalbumin Polyelectrolyte Complexes for the Production of Oxidation Stable Tuna Oil Microcapsules. *Int. J. Biol. Macromol.* **2024**, *273*, 133139. [CrossRef] [PubMed]
37. Khapre, M.A.; Pandey, S.; Jugade, R.M. Glutaraldehyde-Cross-Linked Chitosan–Alginate Composite for Organic Dyes Removal from Aqueous Solutions. *Int. J. Biol. Macormol.* **2021**, *190*, 862–875. [CrossRef]
38. Niculescu, A.-G.; Grumezescu, A.M. Applications of Chitosan-Alginate-Based Nanoparticles—An Up-to-Date Review. *Nanomaterials* **2022**, *12*, 186. [CrossRef]
39. Casadidio, C.; Peregrina, D.V.; Gigliobianco, M.R.; Deng, S.; Censi, R.; Di Martino, P. Chitin and Chitosans: Characteristics, Eco-Friendly Processes, and Applications in Cosmetic Science. *Mar. Drugs* **2019**, *17*, 369. [CrossRef]
40. Pellis, A.; Guebitz, G.M.; Nyanhongo, G.S. Chitosan: Sources, Processing and Modification Techniques. *Gels* **2022**, *8*, 393. [CrossRef]
41. Aranaz, I.; Alcántara, A.R.; Civera, M.C.; Arias, C.; Elorza, B.; Heras Caballero, A.; Acosta, N. Chitosan: An Overview of Its Properties and Applications. *Polymers* **2021**, *13*, 3256. [CrossRef]
42. Guzmán, E.; Ortega, F.; Rubio, R.G. Chitosan: A Promising Multifunctional Cosmetic Ingredient for Skin and Hair Care. *Cosmetics* **2022**, *9*, 99. [CrossRef]
43. Fernández-Peña, L.; Mojahid, B.Z.E.; Guzmán, E.; Ortega, F.; Rubio, R.G. Performance of Oleic Acid and Soybean Oil in the Preparation of Oil-in-Water Microemulsions for Encapsulating a Highly Hydrophobic Molecule. *Colloids Interfaces* **2021**, *5*, 50. [CrossRef]
44. Song, H.; Taylor, D.C.; Zhang, M. Bioengineering of Soybean Oil and Its Impact on Agronomic Traits. *Int. J. Mol. Sci.* **2023**, *24*, 2256. [CrossRef] [PubMed]
45. Zaaboul, F.; Zhao, Q.; Xu, Y.; Liu, Y. Soybean Oil Bodies: A Review on Composition, Properties, Food Applications, and Future Research Aspects. *Food Hydrocoll.* **2022**, *124*, 107296. [CrossRef]
46. Ormeño-Martínez, M.; Guzmán, E.; Fernández-Peña, L.; Greaves, A.J.; Bureau, L.; Ortega, F.; Rubio, R.G.; Luengo, G.S. Roles of Polymer Concentration and Ionic Strength in the Deposition of Chitosan of Fungal Origin onto Negatively Charged Surfaces. *Biomimetics* **2024**, *9*, 534. [CrossRef] [PubMed]
47. Hernández-Rivas, M.; Guzmán, E.; Fernández-Peña, L.; Akanno, A.; Greaves, A.; Léonforte, F.; Ortega, F.; Rubio, R.G.; Luengo, G.S. Deposition of Synthetic and Bio-Based Polycations onto Negatively Charged Solid Surfaces: Effect of the Polymer Cationicity, Ionic Strength, and the Addition of an Anionic Surfactant. *Colloids Interfaces* **2020**, *4*, 33. [CrossRef]
48. Ravera, F.; Santini, E.; Loglio, G.; Ferrari, M.; Liggieri, L. Effect of Nanoparticles on the Interfacial Properties of Liquid/Liquid and Liquid/Air Surface Layers. *J. Phys. Chem. B* **2006**, *110*, 19543–19551. [CrossRef] [PubMed]
49. Varga, I.; Campbell, R.A. General Physical Description of the Behavior of Oppositely Charged Polyelectrolyte/Surfactant Mixtures at the Air/Water Interface. *Langmuir* **2017**, *33*, 5915–5924. [CrossRef]
50. Guzmán, E.; Maestro, A.; Ortega, F.; Rubio, R.G. Association of Oppositely Charged Polyelectrolyte and Surfactant in Solution: Equilibrium and Nonequilibrium Features. *J. Phys. Cond. Matter* **2023**, *35*, 323001. [CrossRef] [PubMed]
51. Smoluchowski, M. *Handbuch der Elektrizität und des Magnetismus*; Barth: Leipzig, Germany, 1921.
52. Berne, B.J.; Pecora, R. *Dynamic Light Scattering: With Applications to Chemistry, Biology, and Physics*; John Wiley & Sons: New York, NY, USA, 2003.

53. Fernández-Peña, L.; Gutiérrez-Muro, S.; Guzmán, E.; Lucia, A.; Ortega, F.; Rubio, R.G. Oil-In-Water Microemulsions for Thymol Solubilization. *Colloids Interfaces* **2019**, *3*, 64. [CrossRef]
54. Xu, W.; Li, Z.; Li, H.; Sun, H.; Zheng, S.; Luo, D.; Li, Y.; Wang, Y.; Shah, B.R. Stabilization and Microstructural Network of Pickering Emulsion Using Different Xanthan Gum/Lysozyme Nanoparticle Concentrations. *LWT* **2022**, *160*, 113298. [CrossRef]
55. Santini, E.; Guzmán, E.; Ferrari, M.; Liggieri, L. Emulsions Stabilized by the Interaction of Silica Nanoparticles and Palmitic Acid at the Water-Hexane Interface. *Colloids Surf. A* **2014**, *460*, 333–341. [CrossRef]
56. González-González, A.; Sánchez-Arribas, N.; Santini, E.; Rodríguez-Villafuerte, J.L.; Carbone, C.; Ravera, F.; Ortega, F.; Liggieri, L.; Rubio, R.G.; Guzmán, E. Effects of Oil Phase on the Inversion of Pickering Emulsions Stabilized by Palmitic Acid Decorated Silica Nanoparticles. *Colloids Interfaces* **2022**, *6*, 27. [CrossRef]
57. Zhou, B.; Gao, S.; Li, X.; Liang, H.; Li, S. Antioxidant Pickering Emulsions Stabilised by Zein/Tannic Acid Colloidal Particles with Low Concentration. *Int. J. Food Sci. Technol.* **2020**, *55*, 1924–1934. [CrossRef]
58. Luo, S.-Z.; Hu, X.-F.; Pan, L.-H.; Zheng, Z.; Zhao, Y.-Y.; Cao, L.-L.; Pang, M.; Hou, Z.-G.; Jiang, S.-T. Preparation of Camellia Oil-Based W/O Emulsions Stabilized by Tea Polyphenol Palmitate: Structuring Camellia Oil as a Potential Solid Fat Replacer. *Food Chem.* **2019**, *276*, 209–217. [CrossRef]
59. Dong, D.; Hua, Y. Glycinin-Gum Arabic Complex Formation: Turbidity Measurement and Charge Neutralization Analysis. *Food Res. Int.* **2016**, *89*, 709–715. [CrossRef] [PubMed]
60. Nivard, M.; Ortega, F.; Rubio, R.G.; Guzmán, E. Adsorption and Bulk Assembly of Quaternized Hydroxyethylcellulose—Anionic Surfactant Complexes on Negatively Charged Substrates. *Polymers* **2025**, *17*, 207. [CrossRef]
61. Ruano, M.; Mateos-Maroto, A.; Ortega, F.; Ritacco, H.; Rubio, J.E.F.; Guzmán, E.; Rubio, R.G. Fabrication of Robust Capsules by Sequential Assembly of Polyelectrolytes onto Charged Liposomes. *Langmuir* **2021**, *37*, 6189–6200. [CrossRef]
62. Binks, B.P.; Lumsdon, S.O. Transitional Phase Inversion of Solid-Stabilized Emulsions Using Particle Mixtures. *Langmuir* **2000**, *16*, 3748–3756. [CrossRef]
63. Binks, B.P.; Lumsdon, S.O. Catastrophic Phase Inversion of Water-in-Oil Emulsions Stabilized by Hydrophobic Silica. *Langmuir* **2000**, *16*, 2539–2547. [CrossRef]
64. Fernandes Barros, F.M.; Chassenieux, C.; de Souza Lima, M.M.; Benyahia, L. Structure and Rheology during Catastrophic Phase Inversion of Pickering Emulsions Stabilized with Fumed Silica Particles. *Colloids Surf. A* **2020**, *593*, 124630. [CrossRef]
65. Binks, B.P.; Whitby, C.P. Silica Particle-Stabilized Emulsions of Silicone Oil and Water: Aspects of Emulsification. *Langmuir* **2004**, *20*, 1130–1137. [CrossRef] [PubMed]
66. Binks, B.P.; Lumsdon, S.O. Stability of Oil-in-Water Emulsions Stabilised by Silica Particles. *Phys. Chem. Chem. Phys.* **1999**, *1*, 3007–3016. [CrossRef]
67. Binks, B.P.; Philip, J.; Rodrigues, J.A. Inversion of Silica-Stabilized Emulsions Induced by Particle Concentration. *Langmuir* **2005**, *21*, 3296–3302. [CrossRef] [PubMed]
68. Wu, J.; Ma, G. Recent Studies of Pickering Emulsions: Particles Make the Difference. *Small* **2016**, *12*, 4633–4648. [CrossRef]
69. Zhen Zhou, F.; Swinkels, P.J.M.; Wei Yin, S.; Velikov, K.P.; Schall, P. Pickering Stabilization Mechanism Revealed through Direct Imaging of Particles with Tuneable Contact Angle in a Phase-Separated Binary Solvent. *J. Colloid Interface Sci.* **2024**, *662*, 471–478. [CrossRef] [PubMed]
70. Shen, X.; Cao, M. Bicontinuous Interfacially Jammed Emulsion Gels (Bijels): Preparation, Control Strategies, and Derived Porous Materials. *Nanomaterials* **2024**, *14*, 574. [CrossRef] [PubMed]
71. Reeves, M.; Stratford, K.; Thijssen, J.H.J. Quantitative Morphological Characterization of Bicontinuous Pickering Emulsions via Interfacial Curvatures. *Soft Matter* **2016**, *12*, 4082–4092. [CrossRef]